

Peroxyl Radical Mediated Oxidative DNA Base Damage: Implications for Lipid Peroxidation Induced Mutagenesis[†]

Punnajit Lim,[‡] Gerald E. Wuenschell,[‡] Vanessa Holland,[‡] Dong-Hyun Lee,[‡] Gerd P. Pfeifer,[‡] Henry Rodriguez,[§] and John Termini^{*‡}

Division of Molecular Biology and Biology, Beckman Research Institute of the City of Hope, 1450 East Duarte Road, Duarte, California 91010, and Chemical Science and Technology Laboratory, National Institute of Standards and Technology, Building A227/A239, MS 8311, Gaithersburg, Maryland 20899-8311

Received August 10, 2004; Revised Manuscript Received September 23, 2004

ABSTRACT: Endogenous DNA damage induced by lipid peroxidation is believed to play a critical role in carcinogenesis. Lipid peroxidation generates free radical intermediates (primarily peroxyl radicals, ROO•) and electrophilic aldehydes as the principal genotoxicants. Although detailed information is available on the role of aldehyde base adducts in mutagenesis and carcinogenesis, the contribution of peroxyl radical mediated DNA base damage is less well understood. In the present study we have mapped oxidative base damage induced by peroxyl radicals in the *supF* tRNA gene and correlated this information with peroxidation-induced mutations in several human fibroblast cell lines. Nearly identical patterns of oxidative base damage were obtained from reaction of DNA with either peroxidizing arachidonic acid (20:4 ω 6) or peroxyl radicals generated by thermolysis of ABIP in the presence of oxygen. Oxidative base damage primarily occurred at G and C. Transversions at GC base pairs in the *supF* gene were the major base substitution detected in all cell lines. Peroxyl radical induced tandem mutations were also observed. Many mutation hot spots coincided with sites of mapped oxidative lesions, although in some cases hot spots occurred adjacent to the damaged base. Evidence is presented for the involvement of 8-oxodG in the oxidation of DNA by ROO•. These results are used to interpret some key features of previously published mutation spectra induced by lipid peroxidation in human cells.

DNA damage resulting from endogenous lipid peroxidation has been recognized as a contributing factor in carcinogenesis (1, 2). Lipid peroxidation is a free radical chain reaction of polyunsaturated fatty acids initiated by both enzymatic and nonenzymatic processes within cellular membranes. Potential DNA-damaging agents produced include free radical intermediates and electrophilic aldehydes (3, 4). The main chain propagating intermediate of lipid peroxidation is the peroxyl radical (5, 6), remarkable for its exceptionally long half-life ($t_{1/2} \sim$ seconds) (7, 8). The concentration of other lipid radical intermediates, such as carbon and alkoxyl radicals, is negligible during lipid peroxidation; therefore, their role in oxidative DNA damage is assumed to be minimal (5, 9, 10). The potentially important role of peroxyl radicals in lipid peroxidation induced genotoxicity has previously been recognized by Marnett (3), but biochemical details of their involvement in oxidative DNA damage remain to be elucidated. In contrast, the mutagenic and carcinogenic contributions of lipid-derived aldehyde base adducts in DNA have been more thoroughly examined.

Fragmentation of lipid radical intermediates results in the termination of free radical chains with the concomitant

generation of electrophilic aldehydes (4, 11, 12). The reactions of these endogenously generated aldehydes with DNA to form cyclic etheno and propano base adducts have been extensively studied (13–15), and their mutation-inducing potential has been explored in detail (16–19). Elevated levels of etheno and propano DNA base adducts have been observed in humans in response to high intake of polyunsaturated fatty acids (20) and in individuals considered to be at high risk for developing certain kinds of cancers (21, 22).

Yet evidence also suggests that, in addition to alkylation damage, endogenous lipid peroxidation may be a significant source of oxidative DNA damage. In a study involving women considered to be at high risk for breast cancer, increased dietary polyunsaturated fatty acids significantly enhanced the levels of 5-(hydroxymethyl)uracil (5-HmdU)¹ in DNA, an effect which could be suppressed by dietary antioxidants (23, 24). Chemical studies have shown that 5-HmdU is the major product obtained from reaction of peroxyl radicals with thymidine (25), consistent with lipid

¹ Abbreviations: ABIP, 2,2'-azobis[2-(2-imidazolin-2-yl)propane] dihydrochloride; AA, arachidonic acid; LMPCR, ligation-mediated polymerase chain reaction; ESI-MS, electrospray ionization mass spectrometry; CID, collision-induced dissociation; GC-IDMS, gas chromatography–isotope dilution mass spectrometry; SIM, selected ion monitoring; BSTFA, *N,O*-bis(trimethylsilyl)trifluoroacetamide; NER, nucleotide excision repair; COX-2, cyclooxygenase 2; 5-LO, 5-lipoxygenase; 5-MeC, 5-methylcytosine; 8-oxodG, 8-oxo-7-hydro-2'-deoxyguanosine; 5-HmdU, 5-hydroxymethyluracil.

[†] Supported by USPHS Grant GM59219 to J.T.

^{*} To whom correspondence should be addressed. Phone: (626) 301-8169. Fax: (626) 930-5463. E-mail: jtermini@coh.org.

[‡] Beckman Research Institute of the City of Hope.

[§] National Institute of Standards and Technology.

peroxidation induced oxidative DNA damage in these patients. Elevated levels of 8-oxodG have been detected in animal models for Wilson's disease, a cancer-prone syndrome characterized by enhanced cellular lipid peroxidation due to abnormal copper storage (26). Increased oxidative metabolism of polyunsaturated fatty acids by nuclear oxygenases such as cyclooxygenase 2 (COX-2) and 5-lipoxygenase (5-LO) generates lipid peroxyl radical intermediates (27, 28) in close proximity to chromatin. Inflammation-induced expression of COX-2 in a rodent model has been shown to stimulate formation of 8-oxoguanine adducts in DNA (29), an effect which could be suppressed by administration of COX-2-specific inhibitors (30).

To examine in greater detail the spectrum of oxidative base damage induced by reaction of DNA with peroxyl radicals, we have used a variation of the ligation-mediated PCR (LMPCR) technique to map oxidized bases in the *supF* tRNA gene induced by reaction with either peroxidizing AA or peroxyl radicals generated from the decomposition of 2,2'-azobis[2-(2-imidazolin-2-yl)propane] dihydrochloride (ABIP) in the presence of O₂. The mapped oxidative base damage patterns were correlated with mutation hot spots in the *supF* gene acquired in mammalian cells. The full range of guanine lesions which give rise to the observed base substitution mutations is not known; however, quantitative measurement of the time-dependent formation and decay of 8-oxoG in the course of peroxyl radical oxidation of double-stranded DNA suggests its intermediate involvement in lipid peroxidation induced mutagenesis.

MATERIALS AND METHODS

Chemicals and Reagents. Arachidonic acid (AA, 20:4 ω 6) was obtained from Avanti Polar Lipids (Alabaster, AL). Purity was assessed by ESI-MS in the negative ion mode (Mariner Biospectrometry Workstation; Applied Biosystems, Foster City, CA) and was judged to be >98%. Water-soluble diazo initiator 2,2'-azobis[2-(2-imidazolin-2-yl)propane] dihydrochloride (ABIP) was obtained from Wako Chemicals (Richmond, VA).

Sequence Mapping of Oxidative Base Damage. The pSP189 shuttle vector containing the *supF* tRNA gene as a mutational marker was reacted with either peroxidizing AA or peroxyl radicals generated by the thermolysis of ABIP in the presence of O₂. Reactions of pSP189 plasmid DNA with either ABIP/O₂ or peroxidizing arachidonic acid were as previously described (31). Methylated pSP189 was obtained by reaction with SssI methylase in the presence of S-adenosylmethionine, which results in C-5 cytosine methylation at all CpG sites (32). Peroxidized pSP189 was digested with Fpg or Nth proteins under saturating conditions in order to create single strand breaks at oxidized purines or pyrimidines, respectively, prior to mapping by LMPCR (33). An LMPCR protocol for analysis of UV damage in the *supF* gene of pSP189 has recently been described (32) and was modified for the mapping of oxidative base damage. In brief, oligonucleotide primer *supF*-1 (5'-CAAAAAAGGGAATAAGG-3') was annealed to 0.5 μ g of oxidized, enzyme-digested DNA, followed by primer extension at 48 °C with Sequenase 2.0 (USB, Cleveland, OH). The oligonucleotide linker, consisting of a 25-mer annealed to an 11-mer oligonucleotide, was then ligated to the blunt-ended, primer-extended mol-

ecules. DNA fragments were amplified with Taq polymerase (Roche, Indianapolis, IN) using the 25-mer of the linker and a gene-specific PCR primer *supF*-2 (5'-TAAGGGCGA-CACGGAAAT-3'). After 21 cycles of PCR, the samples were phenol-chloroform extracted and ethanol precipitated, and the amplified fragments were separated on 8% (w/v) polyacrylamide gels containing 7 M urea. The samples were run until the xylene cyanol dye reached the bottom of the sequencing gel, and the bottom 40 cm of the gel was electroblotted onto nylon membranes by using an electrotransfer device (Owl Scientific, Cambridge, MA). The sequences were visualized by autoradiography after hybridization with a single-stranded gene-specific PCR probe. The hybridization probes were made by repeated runoff polymerization using primer *supF*-3 (5'-GAAATGTTGAATACT-CATACTCTTCC-3') and the respective PCR products as templates. Fragments created by Maxam-Gilbert sequencing reactions of pSP189 were also amplified by LMPCR and were used to assign oxidized bases within the *supF* tRNA gene and to calibrate signal intensities.

Human Fibroblast Cell Lines. Fibroblasts defective in nucleotide excision repair proteins XPA (GM04429) and XPF (GM08437), as well as DNA repair proficient fibroblasts (GM00637), were obtained from the Coriell Institute for Medical Research (Camden, NJ). Fibroblasts derived from a patient with the XP-G class 2 defect (XP3BR.SV) were provided by Dr. A. Sarasin, Institut Gustave Roussy (Villejuif, France). All cell lines were SV40 immortalized. Cells were cultured in Dulbecco's modified Eagle's high-glucose medium (Irvine Scientific, Santa Ana, CA) and supplemented with 4 mM L-glutamine, 100 units/mL penicillin G, 100 μ g/mL streptomycin (Gibco Invitrogen Corp., Grand Island, NY), and 10% fetal bovine serum (Omega Scientific, Inc., Tarzana, CA). Cells were maintained in a 10% CO₂ atmosphere in a humidified incubator.

Mutagenesis Assay. The shuttle vector pSP189 and *Escherichia coli* (*E. coli*) indicator strain MBM7070 were kindly provided by Dr. Michael Seidman (34). The pSP189 plasmid contains the *supF* amber suppressor tRNA gene as a mutational marker, as well as sequences required for replication in both SV40 permissive mammalian cells and *E. coli*. Plasmid DNA (5 μ g) was reacted with peroxyl radicals generated by thermolysis of ABIP in the presence of O₂ as previously described (31). Oxidized DNA was isolated by ethanol precipitation and immediately used to transfect human cells using the nonliposomal FuGene 6 reagent (Roche Diagnostics, Indianapolis, IN) according to the instructions of the manufacturer. Human fibroblasts were seeded at a density of 6×10^5 cells/100 mm plate 24 h prior to transfection. Cells were allowed to grow for 72 h at 37 °C prior to plasmid isolation using the alkaline lysis method. Unreplicated plasmids were removed by *DpnI* digestion (10 units at 37 °C for 30 min), RNA was removed by RNase digestion, and DNA was recovered by ethanol precipitation with glycogen prior to electroporation (Bio-Rad GenePulser II, Hercules, CA) into *E. coli* MBM7070 indicator strain. Bacteria were plated on LB agar supplemented with carbenicillin (120 μ g/mL), X-gal (120 μ g/mL; 5-bromo-4-chloro-3-indoyl β -D-galactopyranoside), and IPTG (40 μ g/mL; isopropyl β -D-thiogalactopyranoside). The plates were incubated at 37 °C for 12–16 h prior to scoring for normal (blue) or mutant (light blue or white) colonies. Mutation

frequency was calculated as the number of white and light blue/total colonies. Statistical significance was judged using the chi-square test. Plasmid DNA from mutant colonies was isolated and sequenced as previously described (31).

Quantification of 8-Oxoguanine in Calf Thymus DNA by Gas Chromatography–Isotope Dilution Mass Spectrometry (GC-IDMS). Calf thymus DNA (100 ng) was dissolved in 300 μ L of 10 mM sodium phosphate buffer, pH 7.4, prior to the addition of 34 μ L of a 1 mM solution of ABIP. Reactions were maintained at 40 °C under an atmosphere of O₂ in a Parr reactor with continuous shaking. Oxidations were stopped by ethanol precipitation at various time points. The supernatant was decanted, and the DNA pellets were washed two times with 300 μ L of cold 70% EtOH and dried in a SpeedVac (Savant, Irvine, CA). Analysis of oxidatively modified bases in DNA by GC-IDMS using Fpg hydrolysis has previously been described in detail (35). Briefly, dried oxidized DNA samples were dissolved in 100 μ L of sodium phosphate buffer (final concentration 50 mM, pH 7.4) containing 100 mM KCl, 1 mM EDTA, and 0.1 mM dithiothreitol. Following addition of Fpg, three replicates of each sample were incubated at 37 °C. Following incubation, DNA was precipitated with cold ethanol at –20 °C for 2 h. An aliquot of 8-OH-Gua-¹⁵N₃-¹³C (2 pmol) was added as an internal standard to each sample. Samples were centrifuged at 15000g for 30 min at 4 °C. DNA pellets and supernatant fractions were separated. Ethanol was removed from supernatant fractions under vacuum in a SpeedVac. The supernatant fractions were lyophilized for 18 h and then derivatized with 0.6 mL of a 1:1 (v/v) mixture of BSTFA [*N,O*-bis(trimethylsilyl)trifluoroacetamide] and pyridine at room temperature for 2 h under nitrogen. The samples were centrifuged at 5000g for 30 min to precipitate the salt. The clear supernatant fractions were removed and placed in nitrogen-purged vials and tightly sealed with septa. The derivatized samples were analyzed by GC-IDMS with selected ion monitoring (SIM) using a gas chromatograph (Hewlett-Packard Model 5890 Series II)—mass spectrometer (Hewlett-Packard Model 5989A MS Engine) system equipped with an automatic sampler. SIM was performed in the electron ionization mode at 70 eV using the characteristic ions of the trimethylsilyl derivatives of 8-OH-Gua, guanine, and their stable isotope-labeled analogues (36, 37). An aliquot of each sample (4 μ L) was injected into the injection port of the gas chromatograph using the split mode of injection with a ratio of 10 to 1.

RESULTS

Sequence Specificity of Oxidative Base Damage in the *supF* Gene Induced by ABIP/O₂ and Arachidonic Acid. Oxidative DNA damage induced by reaction with ABIP/O₂ or peroxidizing AA (20:4 ω 6) was mapped along the *supF* gene of the pSP189 shuttle vector. Single strand breaks were created at oxidized bases by incubation with Fpg and Nth proteins, which recognize and cleave at a wide variety of oxidized purines and pyrimidines but not at aldehyde base adducts (38–41). The location of these breaks was then determined using ligation-mediated PCR (LMPCR). Oxidative base mapping results for the *supF* tRNA gene in pSP189 are presented in Figure 1. Plasmids were exposed to either pure peroxyl radicals generated from the ABIP/O₂ reaction (Figure 1A) or peroxidizing arachidonic acid (Figure 1B).

The complete sequence of the *supF* coding strand is provided in the peroxyl radical induced base substitution map of Figure 2. Oxidative base mapping was also carried out for 5-methylcytosine (5-MeC) containing pSP189 DNA treated with ABIP/O₂ (Figure 1A, lane 5). Previous work in our laboratory demonstrated that the 5-Me group of thymidine was preferentially oxidized by peroxyl radicals (25). This suggested that C-5 methylation at CpG sites in DNA might enhance the potential for peroxyl radical mediated DNA damage, relative to unmethylated cytosines.

A comparison of the oxidative base damage patterns for unmethylated DNA exposed to either ABIP/O₂ (Figure 1A, lane 6) or AA for 4 or 8 h (Figure 1B, lanes 5 and 6) reveals nearly identical sequence specificities of oxidative damage. Base oxidation occurred primarily at guanines and cytosines. Eight out of 22 guanines (45%) and 5 out of 28 cytosines (18%) within the *supF* tRNA coding strand were detected as oxidized following treatment with either AA or ABIP/O₂. Although observed at weaker intensities, 4 adenines were found to be oxidized in the AA-induced damage pattern in Figure 1B (A_{63,64,86,93}). Lipid peroxidation induced oxidation of adenines has not been previously described. Adenine oxidation was barely detectable in the ABIP/O₂-induced damage pattern, perhaps as a result of the shorter reaction times used (1 h). No oxidative modifications at thymidines were detected in the *supF* tRNA coding strand, although minor reaction at two thymidines was observed in the noncoding strand (see Supporting Information). The results presented in Figure 1B provide the first direct demonstration of sequence-specific oxidative base damage in double-stranded DNA induced by polyunsaturated fatty acid peroxidation.

Treatment of pSP189 with SssI methylase and S-adenosylmethionine results in the methylation of six cytosines at CpG sites within the *supF* tRNA sequence (42). Only one methylated cytosine residue (C₈₃) was observed to be oxidized by peroxyl radicals. Histogram analysis revealed a 4-fold increase in signal intensity relative to unmethylated C₈₃ (data not shown). Guanines associated with methylated CpG sites, such as G_{39,43,78,92}, did not display enhanced reactivity toward peroxyl radicals relative to guanines in the corresponding unmethylated sequence.

Peroxyl Radical Induced Mutation Spectra in Human Cells. Mutations induced by peroxyl radical mediated oxidative base damage in the *supF* gene were determined in four genetically distinct human fibroblast cell lines. Three cell lines (XP-A, XP-G, and XP-F) possessed specific defects in nucleotide excision repair (NER). Mutations were also examined in a repair-competent cell line (GM00637). The different classes of induced mutations are summarized in Table 1. Peroxyl radical induced base damage increased the *supF* mutation frequency from 30- to 50-fold over background levels. The vast majority of the induced mutations were single base substitutions. No base insertions were detected among 207 independent mutations, and deletions were observed only in XP-G cells at a low frequency (4%). Tandem base substitutions were elicited in all cell lines.

The distribution of base substitution mutations is presented in Table 2.

The percentage of transition and transversion mutations was remarkably similar across all cell lines, with transversions predominating to the extent of 84–93%. Transversions

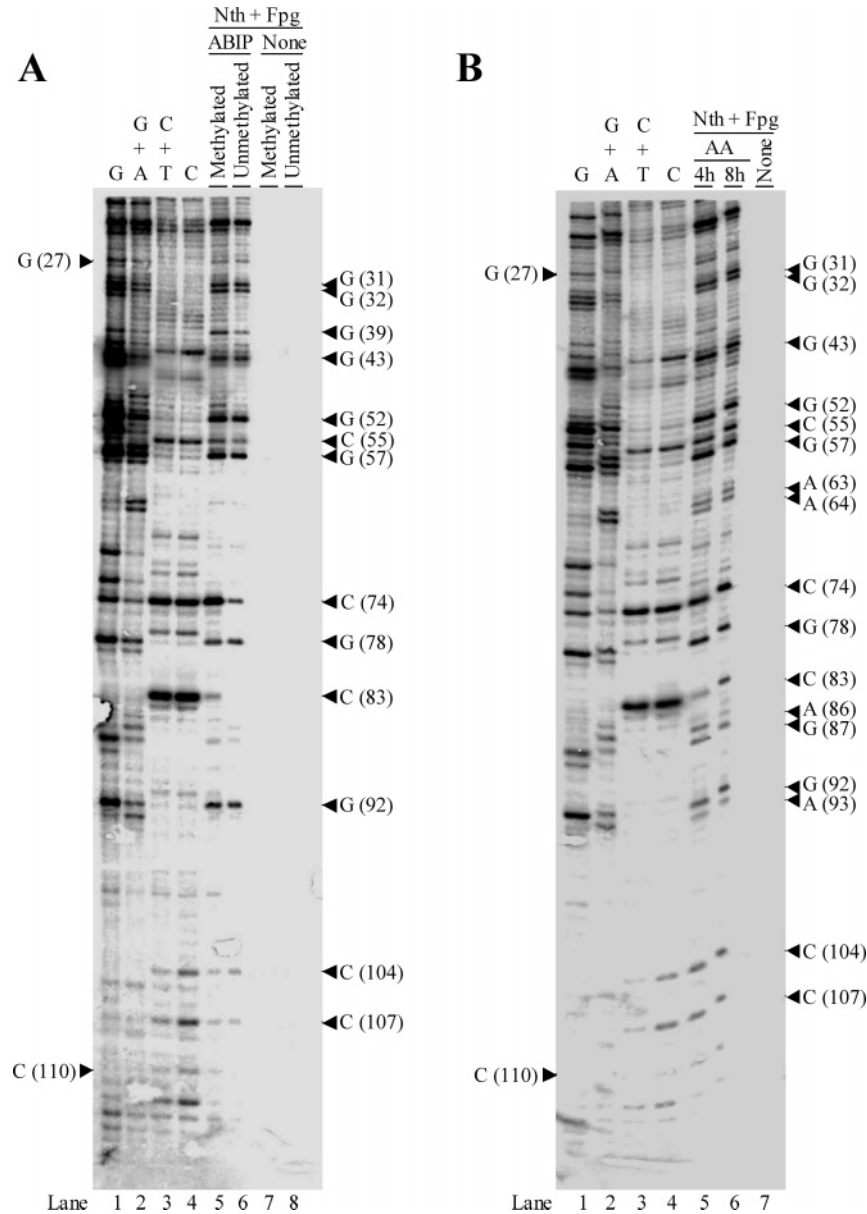


FIGURE 1: Results for oxidative base damage mapping of the coding strand of the *supF* tRNA gene in pSP189. The complete sequence and numbering scheme for *supF* is provided in Figure 2. Lanes 1–4 correspond to Maxam–Gilbert sequencing reactions. Lanes 7 and 8 correspond to unoxidized control pSP189 that was subjected to the mapping protocol. (A) Methylated or unmethylated plasmid DNA (pSP189) was exposed to peroxyl radicals generated by the thermal decomposition of ABIP in the presence of O_2 . (B) Unmethylated pSP189 was reacted with peroxidizing arachidonic acid (AA) for 4 or 8 h.

at GC pairs were the predominant base substitution, whereas AT transversions were detected at a frequency $\leq 5\%$. Transitions consisted almost exclusively of GC/AT substitutions and comprised 5–16% of all base substitutions. The GC transversion distribution consisted of a nearly identical number of GC/TA and GC/CG base substitutions in XP-G and XP-F cell lines. The distribution in the normal fibroblast line was not found to be statistically different from these ratios (chi-square, $P = 0.08$), whereas in the XP-A cells the transversion distribution was more biased toward GC/TA. In general, however, the distribution of mutations was remarkably similar across all cell lines, suggesting that the oxidative base lesions, rather than the cellular repair background, were the primary determinant of the base substitution pattern. A composite map of all peroxyl radical induced *supF* base substitutions is shown in Figure 2. Peroxyl radical induced mutations are displayed above the *supF* coding

strand sequence, while spontaneous (background) mutations are indicated below. More than four base substitutions at any nucleotide position were defined as “hot spots” for mutations. Certain nucleotide positions within the *supF* tRNA sequence were found to be highly prone to base substitution mutations in a manner which was independent of the originating cell line. Peroxyl radical induced tandem mutations are denoted by underlining in Figure 2. A complete list of tandem mutations is provided in Table 3. Eight out of nine tandems were observed at GG, CG, or GT sequence motifs. Identical tandem transversions at $G_{51}G_{52}$ (to TT) were observed independently in both XP-G and XP-F cell lines. Different tandem transversions at $G_{72}T_{73}$ were generated in XP-G and normal fibroblasts, consisting of CA and CG base substitutions, respectively.

Quantitation of Peroxyl Radical Induced Formation of 8-OxoG in DNA by GC-IDMS. The predominance of



FIGURE 2: Distribution of base substitution mutations induced by peroxyl radicals in the *supF* tRNA gene of pSP189 following replication in human fibroblasts. The cellular origin of individual base substitutions is indicated by color. Mutations induced by peroxyl radicals appear above the *supF* sequence, while spontaneous (background) mutations are denoted below. Tandem mutations are underlined. Asterisks indicate bases detected as oxidized from the mapping data of Figure 1A.

Table 1: Classification of Peroxyl Radical Induced Mutations in pSP189 Replicated in Human Cells

	cell line			
	normal fibroblast ^a	XP-A	XP-G	XP-F
independent plasmids analyzed	22 (100)	73 (100)	66 (100)	38 (100)
point mutations				
single base substitutions	19 (86)	67 (92)	57 (86)	35 (92)
tandem base substitutions	3 (14)	2 (3)	2 (3)	2 (5)
multiple base substitutions	0	4 (5)	3 (5)	1 (3)
deletions	0	0	3 (4)	0
insertions	0	0	0	0
deletions/insertions	0	0	0	0
others	0	0	1 (2)	0
fold induced mutant fractions ^b				
1 mM ABIP	32×	ND	52×	33×

^a Number of independent plasmids with alterations (%). ^b Relative increase in mutation frequency over spontaneous mutant frequency.

oxidative damage sites and base substitution mutations at G suggested the potential involvement of 8-oxoG and derived secondary oxidation products. Double-stranded DNA was subjected to oxidation by peroxyl radicals and analyzed for the time-dependent formation of 8-oxoG using GC-IDMS. Gas chromatography/mass spectrometry (GC/MS) with selective ion monitoring (SIM) was used to detect 8-oxoG following digestion of peroxidized calf thymus DNA with

Table 2: Distribution of Peroxyl Radical Induced Base Substitution Mutations in pSP189 Replicated in Human Cells

	cell line			
	normal fibroblast ^a	XP-A	XP-G	XP-F
transitions	4 (16)	10 (12)	6 (9)	3 (7)
G•C → A•T	4 (16)	9 (11)	6 (9)	2 (5)
A•T → G•C	0	1 (1)	0	1 (2)
transversions	21 (84)	70 (88)	62 (91)	39 (93)
G•C → T•A	12 (48)	53 (67)	31 (46)	19 (45)
G•C → C•G	7 (28)	16 (20)	29 (43)	17 (41)
A•T → T•A	1 (4)	1 (1)	1 (1)	2 (5)
A•T → C•G	1 (4)	0	1 (1)	1 (2)
total	25 (100)	80 (100)	68 (100)	42 (100)

^a Number of mutations (%).

the Fpg protein. Quantitation was achieved by the isotope dilution method using [¹⁵N₃,¹³C]-8-oxoG as an internal standard (43). The results of these experiments are shown in Figure 3. The level of 8-oxoG in calf thymus DNA was observed to increase from 43/10⁶ bases to 120/10⁶ bases after 4 h of reaction. Increased oxidation times led to a gradual depletion of 8-oxoG. The 8-oxoG lesion density after 48 h of reaction was observed to be slightly lower than the original background levels. These results demonstrate that guanines can be oxidized in double-stranded DNA to 8-oxoG by

Table 3: Peroxyl Radical Induced Tandem Mutations in *supF*

wt <i>supF</i> ^a	tandem mutation	cell line
G ₃₀ G ₃₁	AA	XP-A
G ₃₁ G ₃₂	TT	XP-F
C ₃₈ G ₃₉	AA	XP-A
G ₅₁ G ₅₂	TT	XP-G
G ₅₁ G ₅₂	TT	XP-F
A ₅₈ C ₅₉	TA	normal fibroblast
G ₇₂ T ₇₃	CG	normal fibroblast
G ₇₂ T ₇₃	CA	XP-G
C ₈₃ G ₈₄	AT	normal fibroblast

^a Sequence position of tandem substitution in wild-type *supF*.

peroxyl radicals and that additional oxidative decomposition takes place to yield secondary products.

DISCUSSION

A modification of the LMPCR sequencing method specifically designed to detect oxidized purines and pyrimidines was used to identify DNA base damage sites induced by lipid peroxidation or by peroxyl radicals generated by the ABIP/O₂ reaction. The Fpg and Nth glycosylase/AP lyase proteins used to create strand breaks at lesion sites do not recognize aldehyde-adducted bases, allowing for detailed examination of the oxidative component of lipid peroxidation induced DNA damage. Mapping of oxidative damage within the *supF* tRNA marker gene of pSP189 also provided an opportunity to examine the relationship between base damage and mutations induced by peroxyl radicals in several human cell lines.

The patterns of sequence-specific oxidative base damage induced by either AA or ABIP/O₂ were nearly identical. This suggests that peroxyl radicals are the principle oxidants involved in lipid peroxidation induced base damage in DNA. More reactive and less selective oxidants such as hydroxyl radicals would have given rise to a substantially larger fraction of damage at pyrimidines. For example, oxidative base damage mapping of DNA following reaction with hydrogen peroxide revealed modifications at ~50% of all C and T bases (44). In contrast, reaction with ABIP/O₂ or peroxidizing arachidonic acid resulted in the modification of only 18% of C and <5% of T bases in the *supF* tRNA gene. Peroxyl radicals displayed a marked preference for reaction at G, the most readily oxidized base (45), consistent with their enhanced selectivity.

Out of six CpG methylation sites in *supF*, only one (C₈₃) was detected as oxidized in our assay. Cytosine methylation increased the extent of oxidative damage by 4-fold at C₈₃ in the *supF* tRNA gene relative to the unmethylated base. Whether addition of a 5-Me group in general enhances reactivity of C toward peroxyl radicals cannot be determined from our data. However, increased oxidizability may be possible due to the facile formation of resonance-stabilized benzylic radicals upon 5-Me hydrogen atom abstraction, as previously proposed for reaction of thymidine with peroxyl radicals (25). It was recently shown that cytosine methylation increased the frequency of transition mutations induced by hydrogen peroxide at CpG sites, consistent with increased oxidative damage at 5-Me-C (42).

We undertook an extensive analysis of peroxyl radical induced mutation spectra in the *supF* tRNA gene for

unmethylated pSP189 DNA in several mammalian cell lines. The predominance of transversions at GC sites was similar to previous results obtained for peroxyl radical induced mutations in *E. coli* using the lacZα gene as a reporter (46). The ratio of transversions/transitions was not significantly different between mammalian cell lines, and the distribution of base substitution mutations was strikingly similar for XP-G, XP-F, and normal fibroblasts. Failure to observe significant differences in the level of induction and distribution of base substitution mutations between NER defective and normal cell lines suggested a diminished role for repair of peroxyl radical induced base damage by NER. A significant number of tandem mutations were induced by peroxyl radicals in all human fibroblast cell lines examined. Tandems were not observed in peroxyl radical induced mutation spectra in bacteria (46). Tandem mutations induced by hydroxyl radical induced oxidative damage at CC sites have been previously described by Loeb (47, 48). More recently, tandem mutations involving purines have been recognized as a feature of oxidative DNA damage (31, 49, 50). Nearly half (4/9) of the peroxyl radical induced tandem mutations occurred at GG sequences. This motif has been identified as a hot spot for oxidative damage (51). The formation of 8-oxoG at GG sites lowers the ionization potential of the adjacent guanine (52), enhancing the probability of tandem lesion formation. Since the majority of GG tandem mutations consist of TT transversions (3/4), either 8-oxoG and/or oxazolone may be involved (see below). Box and co-workers initially suggested that sequences of the type G(T/C) were susceptible to oxidative damage and identified 8-oxoG and a formamido remnant as the major products resulting from a single initiating radical event (53). Two tandem mutations were detected at GT sites in our studies (Table 3), but the CG and CA double transversions observed are inconsistent with this lesion composition.

Oxidative base damage mapping data for the *supF* gene in Figure 1A was used to interpret the sequence distribution of peroxyl radical induced mutation hot spots in mammalian cells. In many cases mutagenic hot spots coincided with prominent damage sites (indicated by an asterisk in Figure 2). Mutation hot spots at G_{31,32,39,52,57,92} and C_{74,83,104} coincided with peroxyl radical induced damage sites in the coding strand of *supF*. Other prominent mutation sites at G_{61,67,91,100,103} corresponded to oxidized bases detected in the noncoding strand (see Supporting Information). A few mutation hot spots were observed adjacent to the 5' or 3' side of mapped damage sites, e.g., G₈₄. This phenomenon may be attributable to "action at a distance" mutagenesis, whereby an oxidative lesion induces replication errors at adjacent template sites (54). Polymerase miscoding at both the lesion site and adjacent site would lead to tandem mutations without the requirement for tandem lesion formation. Tandem mutations at G₅₁G₅₂ may have arisen from this mechanism, whereas the tandem at G₃₁G₃₂ can be attributed to adjacent oxidative lesions observed in the mapping data of Figure 1.

Our results indicate that the peroxyl radical is an effective 1e⁻ oxidant for guanine [E_{G[•]/G} = 1.29 V (45)]. A proposed mechanism for the peroxyl radical mediated formation of 8-oxodG is provided in Scheme 1. One-electron oxidation of guanine by peroxyl radicals results in the corresponding radical cation 2, with concomitant formation of the conjugate base of the alkyl hydroperoxide. Alkyl peroxide anions are

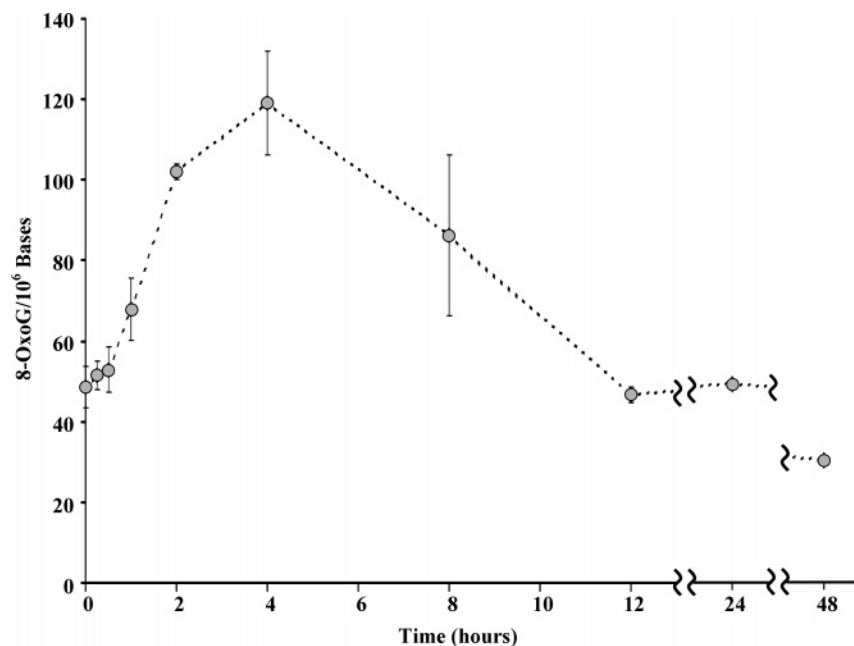
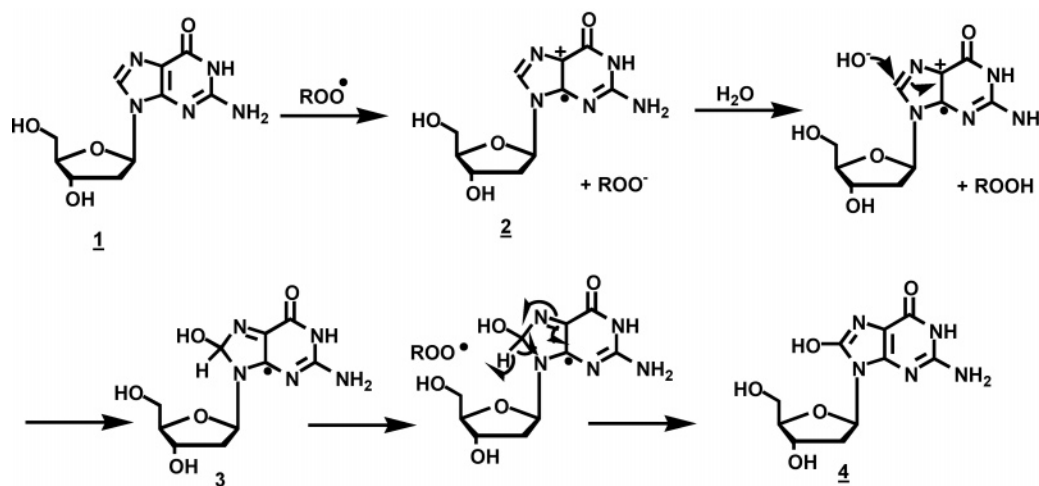


FIGURE 3: Time-dependent quantification of 8-oxoG in calf thymus DNA. Aliquots of reactions of calf thymus DNA with peroxyl radicals were removed at the indicated times, digested with Fpg protein, and analyzed for 8-oxoG using GC-IDMS. Values shown for each time point represent the mean of three determinations.

Scheme 1: Proposed Mechanism for the Formation of 8-OxodG (4) by Peroxyl Radicals



strong bases [$pK_a \sim 13$ (55)] and can deprotonate water in the solvent cage surrounding the radical cation. Attack by ^-OH on **2** provides the neutral radical **3**, which undergoes additional $1e^-$ oxidation and concerted hydrogen abstraction to give 8-oxodG (**4**) shown in the enol form. The enhanced susceptibility of 8-oxoG to secondary oxidation is well-known (52, 56) and is consistent with the time-dependent increase and decay observed in the quantitative MS data of Figure 3. Model compound studies have identified some of these secondary oxidation products resulting from additional $1e^-$ oxidation of 8-oxoG as imidazolone, oxazolone, and guanidinohydantoin (57–59). We have tentatively identified several of these products in the peroxyl radical oxidation of dG nucleoside reactions using ESI-MS/MS fragmentation analyses, in addition to several unidentified products (data not shown). The extent of their distribution in peroxidized double-stranded DNA remains to be determined.

The formation of 8-oxodG in DNA is consistent with the base substitution pattern observed at G in the peroxyl radical

induced *supF* mutation spectra (Figure 2). It is well established that 8-oxoG results in G/T transversions in both bacterial and mammalian cells (60–62). More recently, it has been demonstrated that secondary oxidation products of 8-oxoG such as oxazolone can also induce G/T transversions (63). The identity of the lesion(s) responsible for G/C transversions in the peroxyl radical induced mutation spectrum has not been established; however, other workers have shown that a uniquely substituted guanidinohydantoin in DNA results in the nearly exclusive formation of this base substitution in bacteria (64). Imidazolone, another secondary guanine oxidation product, has also been suggested to be involved in the formation of G/C transversions (58). Thus the majority of the peroxyl radical induced base substitutions observed at G in mammalian cells are consistent with the known coding properties 8-oxoG and derived secondary oxidation products. The base mapping data of Figure 1 were also used to evaluate the contribution of oxidative base damage to the recently reported mutation spectra induced

by arachidonic acid (31). Several oxidative lesion sites identified in Figure 1 correspond to previously observed mutagenic hot spots induced by AA. Examples may be found at G_{57,78} and C_{74,83}. Five out of eight base substitutions at G₅₇ in the AA-induced mutation spectra were G/C and G/T transversions, consistent with oxidative lesions at these sites. Mutations induced at C₈₃ by peroxidizing AA (31) consisted almost entirely of C/T transitions (6/7). Possible candidate oxidative lesions include 5-hydroxycytosine, 5-hydroxyuracil, and uracil glycol (65, 66). More definitive correlations must await the outcome of structural studies of peroxyl radical induced cytosine oxidation products.

Although reaction with either ABIP/O₂ or peroxidizing AA induced oxidative damage at the same G sites in *supF*, the distribution of induced base substitution mutations differed for these two treatments. The ratio of G/T to G/C transversions in XP-G cells was either 1:1 (Table 2) or 4:1 (31) depending upon whether pSP189 was reacted with ABIP/O₂ or AA, respectively. The decreased frequency of G/C transversions in the AA-induced spectra may be attributable to a lower abundance of secondary 8-oxodG oxidation products. These differences may be due to variation in the encounter rate of cationic ABIP peroxyl radicals relative to their neutral or anionic lipid counterparts with DNA. Cationic peroxyl radicals generated by ABIP/O₂ are likely to be associated with the phosphodiester backbone, and thus their participation in successive 1e⁻ base oxidations is entropically favored. The influence of peroxyl radical charge on the yield of DNA strand breaks has been pointed out by Ingold and co-workers (67), and we suggest that similar effects may influence the formation of base oxidation products. Thus 8-oxoG initially formed in DNA via 1e⁻ oxidation by fatty acid derived peroxyl radicals is less likely to undergo secondary oxidation to guanidinohydantoin or other products which induce G/C transversions (58). Despite apparent reactivity differences due to charge, lipid peroxyl radicals are efficient DNA oxidants, capable of inducing both strand breaks and base modifications (31). In addition to the well-known genotoxic effects resulting from the production of electrophilic aldehydes during lipid peroxidation, DNA base oxidation and phosphodiester backbone cleavage by peroxyl radicals must also be considered to be potentially important sources of premutagenic DNA damage.

ACKNOWLEDGMENT

The experimental assistance of Kianoush Sadre-Bazzaz in the mutagenesis experiments is gratefully acknowledged. We thank Dr. P. K. C. Cooper (University of California, Berkeley) for the gift of XP-G fibroblasts. Certain commercial equipment or materials are identified in this paper in order to specify adequately the experimental procedures. Such identification does not imply recommendation or endorsement by the National Institute of Standards and Technology, nor does it imply that the materials or equipment identified are necessarily the best available for the purpose.

SUPPORTING INFORMATION AVAILABLE

A figure showing the oxidative base mapping results for the noncoding strand of the *supF* tRNA gene. This material is available free of charge via the Internet at <http://pubs.acs.org>.

REFERENCES

- Marnett, L. J., and Plataras, J. P. (2001) Endogenous DNA damage and mutation, *Trends Genet.* 17, 214–221.
- Bartsch, H., Nair, J., and Owen, R. W. (1999) Dietary polyunsaturated fatty acids and cancers of the breast and colorectum: emerging evidence for their role as risk modifiers, *Carcinogenesis* 20, 2209–2218.
- Marnett, L. J. (1987) Peroxyl free radicals: potential mediators of tumor initiation and promotion, *Carcinogenesis* 8, 1365–1373.
- Esterbauer, H., Schaur, R. J., and Zollner, H. (1991) Chemistry and biochemistry of 4-hydroxynonenal, malonaldehyde and related aldehydes, *Free Radical Biol. Med.* 11, 81–128.
- Gardner, H. W. (1989) Oxygen radical chemistry of polyunsaturated fatty acids, *Free Radical Biol. Med.* 7, 65–86.
- Barclay, L. R. C., and Ingold, K. U. (1981) Autoxidation of biological molecules. 2. The autoxidation of a model membrane. A comparison of the autoxidation of egg lecithin phosphatidylcholine in water and chlorobenzene, *J. Am. Chem. Soc.* 103, 6478–6485.
- Hildenbrand, K., and Schulte-Frohlinde, D. (1997) Time-resolved EPR studies on the reaction rates of peroxyl radicals of poly(acrylic acid) and of calf thymus DNA with glutathione. Re-examination of a rate constant for DNA, *Int. J. Radiat. Biol.* 71, 377–385.
- Jones, G. D., and O'Neill, P. (1990) The kinetics of radiation-induced strand breakage in polynucleotides in the presence of oxygen: a time-resolved light-scattering study, *Int. J. Radiat. Biol.* 57, 1123–1139.
- Marnett, L. J., and Wilcox, A. L. (1995) The chemistry of lipid alkoxyl radicals and their role in metal-amplified lipid peroxidation, *Biochem. Soc. Symp.* 61, 65–72.
- Maillard, B., Ingold, K. U., and Scaiano, J. C. (1983) Rate constants for the reactions of free radicals with oxygen in solution, *J. Am. Chem. Soc.* 105, 5095–5099.
- Frankel, E. N. (1983) Volatile lipid oxidation products, *Prog. Lipid Res.* 22, 1–33.
- Schneider, C., Tallman, K. A., Porter, N. A., and Brash, A. R. (2001) Two distinct pathways of formation of 4-hydroxynonenal. Mechanisms of nonenzymatic transformation of the 9- and 13-hydroperoxides of linoleic acid to 4-hydroxyalkenals, *J. Biol. Chem.* 276, 20831–20838.
- Marnett, L. J. (1999) Lipid peroxidation-DNA damage by malondialdehyde, *Mutat. Res.* 424, 83–95.
- Chung, F. L., Nath, R. G., Nagao, M., Nishikawa, A., Zhou, G. D., and Randerath, K. (1999) Endogenous formation and significance of 1,N2-propanodeoxyguanosine adducts, *Mutat. Res.* 424, 71–81.
- Nair, J., Barbin, A., Velic, I., and Bartsch, H. (1999) Etheno DNA-base adducts from endogenous reactive species, *Mutat. Res.* 424, 59–69.
- Cheng, K. C., Preston, B. D., Cahill, D. S., Dosanjh, M. K., Singer, B., and Loeb, L. A. (1991) The vinyl chloride DNA derivative N2,3-ethenoguanine produces G → A transitions in *Escherichia coli*, *Proc. Natl. Acad. Sci. U.S.A.* 88, 9974–9978.
- Basu, A. K., Wood, M. L., Niedernhofer, L. J., Ramos, L. A., and Essigmann, J. M. (1993) Mutagenic and genotoxic effects of three vinyl chloride-induced DNA lesions: 1,N6-ethenoadenine, 3,N4-ethenocytosine, and 4-amino-5-(imidazol-2-yl)imidazole, *Biochemistry* 32, 12793–12801.
- Pandya, G. A., and Moriya, M. (1996) 1,N6-ethenodeoxyadenosine, a DNA adduct highly mutagenic in mammalian cells, *Biochemistry* 35, 11487–11492.
- Fink, S. P., Reddy, G. R., and Marnett, L. J. (1997) Mutagenicity in *Escherichia coli* of the major DNA adduct derived from the endogenous mutagen malondialdehyde, *Proc. Natl. Acad. Sci. U.S.A.* 94, 8652–8657.
- Hagenlocher, T., Nair, J., Becker, N., Korfmann, A., and Bartsch, H. (2001) Influence of dietary fatty acid, vegetable, and vitamin intake on etheno-DNA adducts in white blood cells of healthy female volunteers: a pilot study, *Cancer Epidemiol. Biomarkers Prev.* 10, 1187–1191.
- Schmid, K., Nair, J., Winde, G., Velic, I., and Bartsch, H. (2000) Increased levels of promutagenic etheno-DNA adducts in colonic polyps of FAP patients, *Int. J. Cancer* 87, 1–4.
- Leuratti, C., Watson, M. A., Deag, E. J., Welch, A., Singh, R., Gottschalg, E., Marnett, L. J., Atkin, W., Day, N. E., Shuker, D. E., and Bingham, S. A. (2002) Detection of malondialdehyde DNA adducts in human colorectal mucosa: relationship with diet and

- the presence of adenomas, *Cancer Epidemiol. Biomarkers Prev.* 11, 267–273.
23. Djuric, Z., Heilbrun, L. K., Reading, B. A., Boomer, A., Valeriote, F. A., and Martino, S. (1991) Effects of a low-fat diet on levels of oxidative damage to DNA to human peripheral nucleated blood cells, *J. Natl. Cancer Inst.* 83, 766–769.
 24. Djuric, Z., Depper, J. B., Uhley, V., Smith, D., Lababidi, S., Martino, S., and Heilbrun, L. K. (1998) Oxidative DNA damage levels in blood from women at high risk for breast cancer are associated with dietary intakes of meats, vegetables, and fruits, *J. Am. Diet Assoc.* 98, 524–528.
 25. Martini, M., and Termini, J. (1997) Peroxyl radical oxidation of thymidine, *Chem. Res. Toxicol.* 10, 234–241.
 26. Yamamoto, F., Kasai, H., Togashi, Y., Takeichi, M., Tomokatsu, H., and Nishimura, S. (1993) Elevated levels of 8-hydroxydeoxyguanosine in DNA of liver, kidneys, and brain of Long-Evans cinnamon rats, *Jpn. J. Cancer Res.* 84, 508–511.
 27. Tang, M. S., Copeland, R. A., and Penning, T. M. (1997) Detection of an Fe²⁺-protoporphyrin-IX intermediate during aspirin-treated prostaglandin H2 synthase II catalysis of arachidonic acid to 15-HETE, *Biochemistry* 36, 7527–7534.
 28. Chamulitrat, W., and Mason, R. P. (1989) Lipid peroxyl radical intermediates in the peroxidation of polyunsaturated fatty acids by lipoxygenase. Direct electron spin resonance investigations, *J. Biol. Chem.* 264, 20968–20973.
 29. Tardieu, D., Jaeg, J. P., Cadet, J., Embvani, E., Corpet, D. E., and Petit, C. (1998) Dextran sulfate enhances the level of an oxidative DNA damage biomarker, 8-oxo-7,8-dihydro-2'-deoxyguanosine, in rat colonic mucosa, *Cancer Lett.* 134, 1–5.
 30. Tardieu, D., Jaeg, J. P., Deloly, A., Corpet, D. E., Cadet, J., and Petit, C. R. (2000) The COX-2 inhibitor nimesulide suppresses superoxide and 8-hydroxy-deoxyguanosine formation, and stimulates apoptosis in mucosa during early colonic inflammation in rats, *Carcinogenesis* 21, 973–976.
 31. Lim, P., Sadre-Bazzaz, K., Shurter, J., Sarasin, A., and Termini, J. (2003) DNA damage and mutations induced by arachidonic acid peroxidation, *Biochemistry* 42, 15036–15044.
 32. Lee, D. H., and Pfeifer, G. P. (2003) Deamination of 5-methylcytosines within cyclobutane pyrimidine dimers is an important component of UVB mutagenesis, *J. Biol. Chem.* 278, 10314–10321.
 33. Rodriguez, H., Valentine, M. R., Holmquist, G. P., Akman, S. A., and Termini, J. (1999) Mapping of peroxyl radical induced damage on genomic DNA, *Biochemistry* 38, 16578–16588.
 34. Kraemer, K. H., and Seidman, M. M. (1989) Use of supF, an *Escherichia coli* tyrosine suppressor tRNA gene, as a mutagenic target in shuttle-vector plasmids, *Mutat. Res.* 220, 61–72.
 35. Rodriguez, H., Jurado, J., Laval, J., and Dizdaroglu, M. (2000) Comparison of the levels of 8-hydroxyguanine in DNA as measured by gas chromatography mass spectrometry following hydrolysis of DNA by *Escherichia coli* Fpg protein or formic acid, *Nucleic Acids Res.* 28, E75.
 36. Dizdaroglu, M. (1991) Chemical determination of free radical-induced damage to DNA, *Free Radical Biol. Med.* 10, 225–242.
 37. Dizdaroglu, M. (1994) Chemical determination of oxidative DNA damage by gas chromatography–mass spectrometry, *Methods Enzymol.* 234, 3–16.
 38. Boiteux, S., Gajewski, E., Laval, J., and Dizdaroglu, M. (1992) Substrate specificity of the *Escherichia coli* Fpg protein (formamidopyrimidine-DNA glycosylase): excision of purine lesions in DNA produced by ionizing radiation or photosensitization, *Biochemistry* 31, 106–110.
 39. D'Ham, C., Romieu, A., Jaquinod, M., Gasparutto, D., and Cadet, J. (1999) Excision of 5,6-dihydroxy-5,6-dihydrothymine, 5,6-dihydrothymine, and 5-hydroxycytosine from defined sequence oligonucleotides by *Escherichia coli* endonuclease III and Fpg proteins: kinetic and mechanistic aspects, *Biochemistry* 38, 3335–3344.
 40. Dizdaroglu, M., Bauche, C., Rodriguez, H., and Laval, J. (2000) Novel substrates of *Escherichia coli* nth protein and its kinetics for excision of modified bases from DNA damaged by free radicals, *Biochemistry* 39, 5586–5592.
 41. Duarte, V., Gasparutto, D., Jaquinod, M., and Cadet, J. (2000) In vitro DNA synthesis opposite oxazolone and repair of this DNA damage using modified oligonucleotides, *Nucleic Acids Res.* 28, 1555–1563.
 42. Lee, D. H., O'Connor, T. R., and Pfeifer, G. P. (2002) Oxidative DNA damage induced by copper and hydrogen peroxide promotes CG → TT tandem mutations at methylated CpG dinucleotides in nucleotide excision repair-deficient cells, *Nucleic Acids Res.* 30, 3566–3573.
 43. Dizdaroglu, M., Jaruga, P., and Rodriguez, H. (2001) Measurement of 8-hydroxy-2'-deoxyguanosine in DNA by high-performance liquid chromatography–mass spectrometry: comparison with measurement by gas chromatography–mass spectrometry, *Nucleic Acids Res.* 29, E12.
 44. Rodriguez, H., Holmquist, G. P., D'Agostino, R., Jr., Keller, J., and Akman, S. A. (1997) Metal ion-dependent hydrogen peroxide-induced DNA damage is more sequence specific than metal specific, *Cancer Res.* 57, 2394–2403.
 45. Steenken, S., and Jovanovic, S. V. (1997) How easily oxidizable is DNA? One electron reduction potentials of adenosine and guanosine radicals in aqueous solution, *J. Am. Chem. Soc.* 119, 617–618.
 46. Valentine, M. R., Rodriguez, H., and Termini, J. (1998) Mutagenesis by peroxyl radical is dominated by transversions at deoxyguanosine: evidence for the lack of involvement of 8-oxo-dG1 and/or abasic site formation, *Biochemistry* 37, 7030–7038.
 47. Reid, T. M., and Loeb, L. A. (1993) Tandem double CC → TT mutations are produced by reactive oxygen species, *Proc. Natl. Acad. Sci. U.S.A.* 90, 3904–3907.
 48. Newcomb, T. G., Allen, K. J., Tkeshelashvili, L., and Loeb, L. A. (1999) Detection of tandem CC → TT mutations induced by oxygen radicals using mutation-specific PCR, *Mutat. Res.* 427, 21–30.
 49. Delatour, T., Douki, T., Gasparutto, D., Brochier, M. C., and Cadet, J. (1998) A novel vicinal lesion obtained from the oxidative photosensitization of TpdG: characterization and mechanistic aspects, *Chem. Res. Toxicol.* 11, 1005–1013.
 50. Maccubbin, A. E., Iijima, H., Ersing, N., Dawidzik, J. B., Patrzyc, H. B., Wallace, J. C., Budzinski, E. E., Freund, H. G., and Box, H. C. (2000) Double-base lesions are produced in DNA by free radicals, *Arch. Biochem. Biophys.* 375, 119–123.
 51. Kino, K., Saito, I., and Sugiyama, H. (1998) Product analysis of GG-specific photooxidation of DNA via electron transfer: 2-aminoimidazolone as a major guanine oxidation product, *J. Am. Chem. Soc.* 120, 7373–7374.
 52. Prat, F., Houk, K. N., and Foote, C. S. (1998) Effect of guanine stacking on the oxidation of 8-oxoguanine in B-DNA, *J. Am. Chem. Soc.* 120, 845–846.
 53. Budzinski, E. E., Maccubbin, A. E., Freund, H. G., Wallace, J. C., and Box, H. C. (1993) Characterization of the products of dinucleoside monophosphates d(GpN) irradiated in aqueous solutions, *Radiat. Res.* 136, 171–177.
 54. Efrati, E., Tocco, G., Eritja, R., Wilson, S. H., and Goodman, M. F. (1999) "Action-at-a-distance" mutagenesis. 8-oxo-7,8-dihydro-2'-deoxyguanosine causes base substitution errors at neighboring template sites when copied by DNA polymerase beta, *J. Biol. Chem.* 274, 15920–15926.
 55. Everett, A. J., and Minkoff, G. J. (1953) The dissociation constants of some alkyl and acyl hydroperoxides, *Trans. Faraday Soc.* 49, 410–414.
 56. Sheu, C., and Foote, C. S. (1995) Reactivity towards singlet oxygen of a 7,8-dihydro-8-oxoguanosine ("8-hydroxyguanosine") formed by photooxidation of a guanosine derivative, *J. Am. Chem. Soc.* 117, 6439–6442.
 57. Adam, W., Saha-Moller, C. R., and Schonberger, A. (1996) Photooxidation of 8-oxo-7,8-dihydro-2'-deoxyguanosine by thermally generated triplet excited ketones from 3-(hydroxymethyl)-3,4,4-trimethyl-1,2-dioxetane and comparison with Type I and Type II photosensitizers, *J. Am. Chem. Soc.* 118, 9233–9238.
 58. Kino, K., and Sugiyama, H. (2001) Possible cause of G–C → C–G transversion mutation by guanine oxidation product, imidazolone, *Chem. Biol.* 8, 369–378.
 59. Luo, W., Muller, J. G., Rachlin, E. M., and Burrows, C. J. (2001) Characterization of hydantoin products from one-electron oxidation of 8-oxo-7,8-dihydroguanosine in a nucleoside model, *Chem. Res. Toxicol.* 14, 927–938.
 60. Cheng, K. C., Cahill, D. S., Kasai, H., Nishimura, S., and Loeb, L. A. (1992) 8-Hydroxyguanine, an abundant form of oxidative DNA damage, causes G–T and A–C substitutions, *J. Biol. Chem.* 267, 166–172.
 61. Wood, M. L., Esteve, A., Morningstar, M. L., Kuziemko, G. M., and Essigmann, J. M. (1992) Genetic effects of oxidative DNA damage: comparative mutagenesis of 7,8-dihydro-8-oxoguanine and 7,8-dihydro-8-oxoadenine in *Escherichia coli*, *Nucleic Acids Res.* 20, 6023–6032.

62. Moriya, M. (1993) Single-stranded shuttle phagemid for mutagenesis studies in mammalian cells: 8-oxoguanine in DNA induces targeted G•C → T•A transversions in simian kidney cells, *Proc. Natl. Acad. Sci. U.S.A.* 90, 1122–1126.
63. Henderson, P. T., Delaney, J. C., Gu, F., Tannenbaum, S. R., and Essigmann, J. M. (2002) Oxidation of 7,8-dihydro-8-oxoguanine affords lesions that are potent sources of replication errors in vivo, *Biochemistry* 41, 914–921.
64. Henderson, P. T., Delaney, J. C., Muller, J. G., Neeley, W. L., Tannenbaum, S. R., Burrows, C. J., and Essigmann, J. M. (2003) The hydantoin lesions formed from oxidation of 7,8-dihydro-8-oxoguanine are potent sources of replication errors in vivo, *Biochemistry* 42, 9257–9262.
65. Kreutzer, D. A., and Essigmann, J. M. (1998) Oxidized, deaminated cytosines are a source of C → T transitions in vivo, *Proc. Natl. Acad. Sci. U.S.A.* 95, 3578–3582.
66. Feig, D. I., Sowers, L. C., and Loeb, L. A. (1994) Reverse chemical mutagenesis: identification of the mutagenic lesions resulting from reactive oxygen species-mediated damage to DNA, *Proc. Natl. Acad. Sci. U.S.A.* 91, 6609–6613.
67. Paul, T., Young, M. J., Hill, I. E., and Ingold, K. U. (2000) Strand cleavage of supercoiled DNA by water-soluble peroxy radicals. The overlooked importance of peroxy radical charge, *Biochemistry* 39, 4129–4135.

BI048276X